Estimation of airship states and model uncertainties using nonlinear estimators

Muhammad Wasim [a], Ahsan Ali [b], Muhammad Mateen Afzal Awan [c, *], Inam ul Hasan Shaikh [b]

[a] *Department of Aeronautics and Astronautics Engineering, Institute of Space Technology, Islamabad Pakistan*

[b] *Department of Electrical Engineering, University of Engineering and Technology, Taxila Pakistan*

[c] *Department of Electrical Engineering, University of Management and Technology, Sialkot Pakistan*

[*] Corresponding author: Muhammad Mateen Afzal Awan Email: mateen.afzal@skt.umt.edu.pk

K E Y W O R D S	A B S T R A C T
	This Airships are lighter than air vehicles and due to their growing number of applications, they are becoming attractive for the research community. Most of the applications require an airship autonomous flight controller which needs an accurate model and state information. Usually, airship states are affected by noise and states information can be lost in the case of sensor's faults, while airship model is affected by model inaccuracies and model uncertainties. This paper presents the application of nonlinear and Bayesian estimators for estimating the states and model uncertainties of neutrally buoyant airship. It is considered that minimum sensor measurements are available, and data is corrupted with process and measurement noise. A novel lumped model uncertainty estimation approach is formulated where airship model is augmented with six extra state variables capturing the model uncertainty of the airship. The designed estimator estimates the airship model uncertainty along with its states. Nonlinear estimators, Extended Kalman Filter and Unscented Kalman Filter are designed for estimating airship attitude, linear velocities, angular velocities and model uncertainties. While Particle filter is designed for the estimation of airship attitude, linear velocities and angular velocities. Simulations have been performed using nonlinear 6-DOF simulation model of experimental airship for assessing the estimator performances. $1 - \sigma$ uncertainty bound and error analysis have been performed for the validation. A comparative study of the estimator's performances is also carried out.

1. Introduction

In the last couple of decades due to the advancement in technology, once again airships are becoming a potential candidate for many applications like communication, surveillance, agriculture, search and rescue, geological exploration, advertisement, conducting archeological surveys, environmental monitoring, heavy cargo lifting and hovering payload deliveries etc. [1]. In order to

successfully use the airship for these applications, it is required to develop its reliable autonomous control.

For airship autonomous control, many control methods have been proposed in the literature for example error-based controllers [2], model based optimal controllers [3], model based nonlinear controllers [4-6] and intelligent controllers [7]. These controllers rely on sensor measurements as a feedback

and some of them require an accurate model information. Therefore, controller performance depends on model accuracy, sensor measurements and sensor functionality. Inertial Navigation System (INS) is used as a sensor suite for air vehicle navigation. INS use Inertial Measurement Unit (IMU) and GPS for identifying position and current attitude of the air vehicle. INS provide excellent accuracy to position and attitude measurements with coverage, but the data obtained is usually affected by noise. Additionally, if the sensor gets stuck due to some fault then the measurements do not remain reliable. To sort out these problems, nonlinear estimators can be a possible remedy as they are able to smooth the measurements obtained by sensors and can estimate states under sensor faults [8].

In nonlinear estimators, variants of Kalman Filters in the form of Extended Kalman Filter (EKF) and Unscented Kalman Filter (UKF) have enjoyed widespread popularity in several applications. Both EKF and UKF use standard Kalman form for post-updates but differ in the propagation of covariance and premeasurement updates. Apart from these, Particle Filter (PF) has also been a state estimator of choice in UAV applications [9]. Particle filter is based on Monte Carlo simulation and it is also known as optimal recursive Bayesian filtering method. It uses conditional probability distribution to generate samples of independent random variables. PF is well suited for high-dimensional problems. Additionally, it can handle non-Gaussian and nonlinear model [10].

In [11], airship attitude, center of mass with respect to center of buoyancy and mass difference between system and displaced air is estimated using discrete time invariant Kalman filter. In [12], a UKF has been applied for spacecraft attitude estimation. In both the above works, gyro sensors are utilized for obtaining attitude measurements and then EKF and UKF are incorporated for smoothing the measured signals. Variants of Kalman filters have been extensively used for attitude estimation of airships, spacecrafts and other Unmanned Aerial Vehicles (UAVs). For comprehensive review the reader is referred to [13,14]. In [15], IMU and GPS measurements are utilized for estimating airship attitude, velocity and position using EKF. In [16], same estimations are made using EKF while utilizing gyro coupled with GPS for position and attitude measurements. In their work they concluded that two EKFs running in sequence outperform a single filter. In this configuration first filter estimates attitude and second filter uses this measurement and estimates

velocity and position. Implementation of EKF requires calculation of Jacobian matrix at each sampling instant which increases its computational cost. In [17], a scheduled EKF has been introduced for airship states and wind velocity estimation under time varying wind condition. In this approach, the Jacobian matrix is precalculated for different airship flight modes. The proposed scheduled law provides the needed Jacobian to the EKF. In [18,40], EKF and UKF are proposed for airship states and aerodynamic coefficient and aerodynamic forces and torques estimation. In [19], UKF is utilized for attitude estimation of airship. In [17-19], sensor measurements in the form of attitude, position and angular velocity have been used as an input by the filter. In our previous work [20-22], it has been demonstrated that Kalman filter can be used for the aerodynamic model estimation of airship also in [22] its utility for model uncertainty estimation is shown.

For airship localization and velocity estimation, PF is reported in [23-25]. In [23-24], probabilistic localization of a miniature indoor airship is done using PF that utilizes lightweight air flow, ultrasound and IMU sensors to approximate the current location of blimp. In [25], an unscented PF is designed for navigation and estimation of airship position in stratosphere in the presence of wind filed disturbance. In the proposed approach, wind speed model is incorporated for PF design. The wind model defines the relationship between airship velocity and wind velocity.

Apart from state estimation, model inaccuracies and model uncertainties also degrade the controller performance. Usually robust controllers are designed to tackle the issue, but high gains may be required for achieving robustness [26]. In [27], it has been demonstrated that if the parameters of segway are calculated online and that information is provided to the controller then the sliding mode controller robustness increases. So, it is practical to estimate model inaccuracies and model uncertainties online and provide that information to the controller. In the literature, different approaches have been proposed for approximating model uncertainties and model inaccuracies. In [28-29], nonlinear disturbance observer is proposed for approximating model uncertainties and external disturbances. In [30-31], adaptive laws based on current and previous state values are proposed. As the proposed adaptive laws are non-decreasing in nature so if the initial bias is too high then they may diverge. In [32-36], Neural Networks (NN) and Radial Basis Function Neural Networks (RBFNNs) and in [37-39], Fuzzy Logic (FL) based techniques are utilized for

dealing with model uncertainties in airship dynamics. The aforementioned methods assume that all current state values of airship are accurately known. Their performance, therefore, degrades under sensor faults and noisy sensor measurements.

Motivated from the above literature, in this work solutions for both problems are proposed. First, an airship states are estimated while considering sensor faults and noisy sensor measurements. It is assumed that airship attitude and angular velocity measuring sensors are faulty and only current inertial position of the airship in the form of x, y and z coordinate is available. In such scenario EKF, UKF and PF are designed for airship attitude, angular velocity and linear velocity estimation based on airship model. Additionally, in order to avoid numerical calculation of Jacobian matrix for EKF, analytical expressions for Jacobian matrix are precalculated so that computational complexity of EKF can be reduced. Second, EKF and UKF are designed for estimating model uncertainties. Existing approaches that deal with model uncertainties assume that the states are accurately known. In the approach proposed in this work, this assumption is dropped. That is, it is assumed that noise and faults are present in the sensors. To deal with sensor faults, a cascaded Kalman filter approach is proposed in which a first Kalman filter uses current position of airship and calculates its attitude. Whereas a second Kalman filter utilizes position and attitude information and estimates airship angular velocities, linear velocities and model uncertainties.

The proposed work makes the following contribution to the existing literature:

1. EKF, UKF and PF are designed for airship state estimation under minimum sensor measurements and sensor faults.

2. A sequential Kalman filtering approach for estimating airship states and its model inaccuracies and uncertainties.
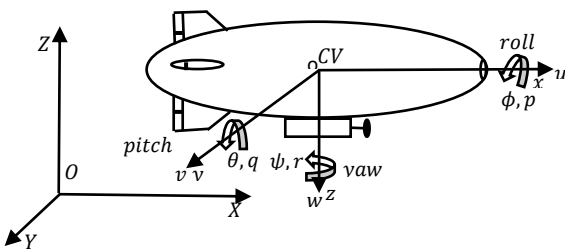

Fig. 1. Airship reference frames

The whole paper is organized in seven sections: In second section, airship complete nonlinear model is explained. Axes conventions, modelling assumptions, kinematic model equations, dynamic model equations and airship model nonlinear state-space representation is given in different sub-sections. In subsection 2.5 airship nominal model is extended by incorporating six additional state variables that captures the modelling inaccuracies, parameter uncertainties and variation of aerodynamic model. In third section, state and measurement functions are introduced for airship state estimation. They are used in estimators design. In forth section, state and measurement functions are introduced for estimating airship model uncertainties. Fifth section discusses the Kalman filter algorithms used in the proposed work. In sixth section, simulation results are given. Two different simulation scenarios are considered. In first case estimator performance for state estimations are discussed. In second case, changes in aerodynamic forces and torques are introduced and EKF and UKF estimations are compared. For comparative study, error analysis is conducted and estimation errors for different estimators are summarized in table. In seventh section, some concluding remarks are given. the door for microgrids. The microgrid concept is established as an alternative solution for electrification for remote areas and as a platform for renewable energy.

2. Airship Modelling

2.1 Axes Convention, States And Modelling Assumptions

Two reference frames are used for the explanation of airship motion. A reference frame that is attached to the airship body having center at the airship Center of Volume (CV) is called the Body Fixed Reference Frame (BFRF) represented by $oxyz$. And second is the Inertial reference Frame (IRF) denoted by $OXYZ$. IRF is located at some point on the earth as shown in the Fig. 1. Propulsion forces (due to the propellers attached on airship gondola) and aerodynamic forces (due to the rudders and elevators) acts on airship in BFRF. However, airship current position and attitudes are assessed with respect to the IRF. So, the simulation environment first calculates the velocities in BFRF and then use transformation matrix to transform them into the IRF the MATLAB based simulation methodology is explained in [40].

Let, airship position and attitude in IRF are represented by $\zeta = [x, y, z]^T$ and $\varsigma = [\phi, \theta, \psi]^T$ respectively and airship linear velocities in BFRF are represented by $v = [u, v, w]^T$ and angular velocities with $\omega = [p, q, r]^T$. Then complete state vector can be

given by $\chi = [\xi^T, v^T]^T$ with $\xi = [\zeta^T, \varsigma^T]^T, v = [v^T, \omega^T]^T$.

Remark 1. Two main propellers are attached to the gondola that moves with the same speed and also vector thrusting is not considered for them. In order to increase yaw movement one propeller is mounted at the tail of airship on the bottom rudder.

Following assumptions are made for deriving 6-DOF airship equations

Assumption 1. The effects of Earth curvature are not considered and the pressure inside the envelope is high enough to maintain the airship as a rigid body.

Assumption 2. The CG lies on the symmetry plane below the CV. The hull is considered as a solid, and aero-elastic phenomena are ignored. The mass of the airship and its volume are considered as constant.

Assumption 3. The Center of Buoyancy (CB) is assumed to coincide with the CV.

2.2 Equations For Airship Kinematic Model

Considering the above defined IRF position and attitude variables and BFRF linear and angular velocities' variables, the vector form of equation for airship kinematic model can be written as:

$$\dot{\xi} = R(\varsigma)v \tag{1}$$

Where

$$R(\varsigma) = \begin{bmatrix} R_1(\varsigma) & O_{3\times3} \\ O_{3\times3} & R_2(\varsigma) \end{bmatrix} \tag{2}$$

With $R_1(\varsigma)$ and $R_2(\varsigma)$ are the rotation matrixes based on Euler angles. $R_1(\varsigma)$, transforms the body axes linear velocities to the inertial frame position derivatives. $R_2(\varsigma)$, transforms the body axes angular velocities into inertial frame attitude derivatives. The expressions for rotation matrixes are given in (3) and (4), where simplified notation is adopted in which sin(.) and cos(.) are replaced by s(.) and c(.).

$R_1(\varsigma) =$
$$\begin{bmatrix} c(\theta)c(\psi) & c(\psi)s(\theta)s(\phi) - c(\phi)s(\psi) & c(\psi)c(\phi)s(\theta) + s(\psi)s(\phi) \\ s(\psi)c(\theta) & c(\psi)c(\phi) + s(\psi)s(\theta)s(\phi) & c(\phi)s(\psi)s(\theta) - s(\phi)c(\psi) \\ -s(\theta) & c(\theta)s(\psi) & c(\theta)c(\psi) \end{bmatrix}$$
$$\tag{3}$$

$$R_2(\varsigma) = \begin{bmatrix} 1 & \tan(\theta)\sin(\phi) & \tan(\theta)\cos(\phi) \\ 0 & \cos(\phi) & -\sin(\phi) \\ 0 & \sin(\phi)\sec(\theta) & \sec(\theta)\cos(\phi) \end{bmatrix} \tag{4}$$

2.3 Equations for airship dynamic model

An extensive literature can be found on airship modelling. The comprehensive review on airship modelling is available in [39]. Airship model can be adopted from the model of buoyancy driven underwater vehicles. [40] summarizes the basic equation of motion for airship. Here the airship model is adopted from [41]. The vector form of equation can write as

$$\dot{V}_b = M^{-1}(F_d + F_{Ad} + F_{As} + F_P) \tag{5}$$

Where, $\dot{V}_b \in \Re^{6\times1}$ is the vector of linear and angular accelerations calculated in BFRF. $M \in \Re^{6\times6}$ is the mass matrix it consists of airship mass and inertia terms. As the displaced air mass due to the airship volume is significant as compared to the airship mass so its effect is not ignored in the formulation of airship equations and added mass and inertia terms are incorporated in airship mass matrix. $F_d \in \Re^{6\times1}$ is a dynamic forces and torques vector. It consists of forces acting on airship due to the Coriolis and centrifugal effects. $F_{Ad} \in \Re^{6\times1}$ is a vector of forces acting on airship due to aerodynamics. In this work airship geometrical parameters are used for the calculation of aerodynamic forces. $F_{As} \in \Re^{6\times1}$ is a vector of forces acting on airship due to the airship weight and buoyancy effects. $F_P \in \Re^{6\times1}$ comprises of forces and torques due to propellers.

2.4 Nonlinear State-Space Representation

Airship model can be represented in nonlinear state space form consisting of twelve state elements as given in (7). This formulation is suitable for estimator design.

Let,

$$f = F_d + F_{Ad} + F_{As} + F_P , f = [f_1, f_2, f_3, f_4, f_5, f_6]^T$$

and

$$M^{-1} = \begin{bmatrix} a_1 & 0 & a_2 & 0 & a_3 & 0 \\ 0 & b_1 & 0 & b_2 & 0 & b_3 \\ a_4 & 0 & a_5 & 0 & a_6 & 0 \\ 0 & b_4 & 0 & b_5 & 0 & b_6 \\ a_7 & 0 & a_8 & 0 & a_9 & 0 \\ 0 & b_7 & 0 & b_8 & 0 & b_9 \end{bmatrix} \tag{6}$$

Using these notations, the nonlinear state space form of airship model will be.

$$\begin{bmatrix} \dot{x} \\ \dot{y} \\ \dot{z} \\ \dot{\phi} \\ \dot{\theta} \\ \dot{\psi} \\ \dot{u} \\ \dot{v} \\ \dot{w} \\ \dot{p} \\ \dot{q} \\ \dot{r} \end{bmatrix} = \begin{bmatrix} c(\psi)c(\theta)u + (c(\psi)s(\phi)s(\theta) - c(\phi)s(\psi))v + (c(\psi)c(\phi)s(\theta) + s(\psi)s(\phi))w \\ s(\psi)c(\theta)u + (s(\psi)s(\phi)s(\theta) + c(\phi)c(\psi))v + (s(\psi)s(\theta)c(\phi) - c(\psi)s(\phi))w \\ -s(\theta)u + (c(\theta)s(\psi))v + (c(\theta)c(\psi))w \\ p + \tan(\theta)\sin(\phi)q + \cos(\phi)\tan(\theta)r \\ \cos(\phi)q - \sin(\phi)r \\ \sec(\theta)\sin(\phi)q + \sec(\theta)\cos(\phi)r \\ a_1f_1 + a_2f_3 + a_3f_5 \\ b_1f_2 + b_2f_4 + b_3f_6 \\ a_4f_1 + a_5f_3 + a_6f_5 \\ b_4f_2 + b_5f_4 + b_6f_6 \\ a_7f_1 + a_8f_3 + a_9f_5 \\ b_7f_2 + b_8f_4 + b_9f_6 \end{bmatrix} \qquad (7)$$

Elements of body axes force vector are mentioned bellow:

$$f_1 = -m_z wq + m_y rv + m[a_x(q^2 + r^2) - a_z rp] +$$
$$\tfrac{1}{2}\rho V_0^2 S[C_{X1}\cos^2(\alpha)\cos^2(\beta) + C_{X2}\sin(\tfrac{\alpha}{2})\sin(2\alpha)$$
$$+ \sin\left(\tfrac{\beta}{2}\right)\sin(2\beta) + C_{X3}] - (W - B)\sin(\theta) + (T_{ds} +$$
$$T_{dp})\cos(\mu) \qquad (8)$$

$$f_2 = -m_x ur + m_z pw + m[-a_x pq - a_z rq] +$$
$$\tfrac{1}{2}\rho V_0^2 S[C_{Y1}\sin(2\beta)\cos\left(\tfrac{\beta}{2}\right) + C_{Y2}\sin(2\beta) +$$
$$C_{Y3}\sin(|\beta|)\sin(\beta) + C_{Y4}(\delta_{RT} + \delta_{RB})] + (W - B)\cos(\theta)\sin(\phi) \qquad (9)$$

$$f_3 = -m_y vp + m_x qu + m[-a_x rp + a_z(q^2 + p^2)] +$$
$$\tfrac{1}{2}\rho V_0^2 S[C_{Z1}\sin(2\alpha)\cos\left(\tfrac{\alpha}{2}\right) + C_{Z2}\sin(2\alpha) +$$
$$C_{Z3}\sin(|\alpha|)\sin(\alpha) + C_{Z4}(\delta_{EL} + \delta_{ER})] + (W - B)\cos(\theta)\cos(\phi) - (T_{ds} + T_{dp})\sin(\mu) \qquad (10)$$

$$f_4 = -(J_z - J_y)rq + J_{xz}pq + ma_z(ur - pw)$$
$$+ \tfrac{1}{2}\rho V_0^2 LS[C_{L1}(\delta_{EL} - \delta_{ER} + \delta_{RB} - \delta_{RT})$$

$$+ C_{L2}\sin(\beta)\sin(|\beta|) + \tfrac{1}{2}\rho S(C_{L3}r|r| + C_{L4}p|p|)] +$$
$$a_z W\cos(\theta)\sin(\phi) + (T_{dp} - T_{ds})\sin(\mu).d_y$$
$$+(T_{ds} + T_{dp})(d_z\cos(\mu) - d_x\sin(\mu)) \qquad (11)$$

$$f_5 = -(J_x - J_z)pr + J_{xz}(r^2 - p^2)$$
$$+ m[a_x(vp - qu) - a_z(wq - rv)]$$
$$+ \tfrac{1}{2}\rho V_0^2 LS[C_{M1}\sin(2\alpha)\cos\left(\tfrac{\alpha}{2}\right)$$
$$+ C_{M2}\sin(2\alpha) + C_{M3}\sin(|\alpha|)\sin(\alpha)$$
$$+ C_{M4}(\delta_{EL} + \delta_{ER}) + \tfrac{1}{2}\rho S(C_{M5}q|q|)]$$
$$- (a_z W - b_z B)\sin(\theta)$$

$$-(a_x W - b_x B)\cos(\theta)\cos(\phi) \qquad (12)$$

$$f_6 = -(J_y - J_x)qp - J_{xz}qr + m[-a_x(ur - pw)] +$$
$$\tfrac{1}{2}\rho V_0^2 LS[C_{N1}\cos\left(\tfrac{\beta}{2}\right)\sin(2\beta) + C_{N2}\sin(2\beta)$$

$$+ C_{N3}\sin(|\beta|)\sin(\beta) + C_{N4}(\delta_{RT} + \delta_{RB}) +$$
$$\tfrac{1}{2}\rho S(C_{N5}r|r|) + a_x W\cos(\theta)\sin(\phi)$$

$$+(T_{dp} - T_{ds})\cos(\mu)d_y \qquad (13)$$

2.5 Modelling Uncertainties In Airship Model

In the case of model uncertainty estimation, for filter formulation, the model state function and model measurement function are modified. In model state function six auxiliary states are introduced for modelling uncertainties. Measuring uncertainty and inaccuracies, lumped approach is adopted. In this approach the auxiliary state variables captures any sort of change in model equations. The change may be due to any parameter variation in the model or inaccurate modelling equations. Airship parameters such as inertia matrix is difficult to measure, and parameter changes may come due to unforeseen shape changes and uneven gas distribution. And modelling inaccuracies in airship model also comes due to unknown aerodynamic model or limitation of wind tunnel experimentation. For testing the proposed lumped approach in current work, a change in aerodynamic model is introduced and the results shows that this change is captured by the auxiliary state variables. In model measurement function, apart from airship position, its attitudes are also utilized. Considering these modifications, the changed equation will be.

$$\dot{V}_b = M^{-1}(F_d + F_{Ad} + F_{As} + F_P) + Mu \qquad (14)$$

Where Mu is six elements column vector that captures model inaccuracies and model uncertainties. Now the complete model of airship accommodating new six states will be

$$
\begin{bmatrix} \dot{x} \\ \dot{y} \\ \dot{z} \\ \dot{\phi} \\ \dot{\theta} \\ \dot{\psi} \\ \dot{u} \\ \dot{v} \\ \dot{w} \\ \dot{p} \\ \dot{q} \\ \dot{r} \\ \dot{M}_{u1} \\ \dot{M}_{u2} \\ \dot{M}_{u3} \\ \dot{M}_{u4} \\ \dot{M}_{u5} \\ \dot{M}_{u6} \end{bmatrix} = \begin{bmatrix} c(\psi)\,c(\theta)\,u + (c(\psi)\,s(\phi)\,s(\theta) - c(\phi)\,s(\psi))v + (c(\psi)\,c(\phi)\,s(\theta) + s(\psi)\,s(\phi))w \\ s(\psi)\,c(\theta)\,u + (s(\psi)\,s(\theta)\,s(\phi) + c(\psi)\,c(\phi))v + (s(\psi)\,s(\theta)\,c(\phi) - c(\psi)\,s(\phi))w \\ -s(\theta)\,u + (c(\theta)\,s(\psi))v + (c(\theta)\,c(\psi))w \\ p + \sin(\phi)\tan(\theta)\,q + \cos(\phi)\tan(\theta)\,r \\ \cos(\phi)\,q - \sin(\phi)\,r \\ \sin(\phi)\sec(\theta)\,q + \cos(\phi)\sec(\theta)\,r \\ a_1 f_1 + a_2 f_3 + a_3 f_5 + M_{u1} \\ b_1 f_2 + b_2 f_4 + b_3 f_6 + M_{u2} \\ a_4 f_1 + a_5 f_3 + a_6 f_5 + M_{u3} \\ b_4 f_2 + b_5 f_4 + b_6 f_6 + M_{u4} \\ a_7 f_1 + a_8 f_3 + a_9 f_5 + M_{u5} \\ b_7 f_2 + b_8 f_4 + b_9 f_6 + M_{u6} \\ 0 \\ 0 \\ 0 \\ 0 \\ 0 \\ 0 \end{bmatrix}
\tag{15}
$$

3. Airship State Estimation

For airship state estimation, the state vector comprises of 12 state elements that have modelling equation given in (7). However, the system is extended by incorporating process noise and measurement noise. The application of Kalman filter algorithm requires that system should be expressed in state-space formulation so, here for airship state estimation following state vector is defined.

$$X = [x \quad y \quad z \quad \phi \quad \theta \quad \psi \quad u \quad v \quad w \quad p \quad q \quad r]^T \tag{16}$$

As for the state estimation, airship current position is used as a measurement, so estimator position estimates are used as a measurement vector given by:

$$Y = CX = \begin{bmatrix} 1 & 0 & 0 & 0 & 0 & 0 & 0 & 0 & 0 & 0 & 0 & 0 \\ 0 & 1 & 0 & 0 & 0 & 0 & 0 & 0 & 0 & 0 & 0 & 0 \\ 0 & 0 & 1 & 0 & 0 & 0 & 0 & 0 & 0 & 0 & 0 & 0 \end{bmatrix} X \tag{17}$$

Eq. 7 represents airship complete nonlinear model it can be compactly represented by the following equation:

$$\dot{X} = f(X, u) \tag{18}$$

For the implementation of discrete time Kalman filter algorithm, first order Euler integration of (18) is performed and the model is also extended with process and measurement noise. The new system representation is given as:

$$X_{k+1} = IX_k + T_s f(X_k, u_k) + w \tag{19}$$

$$Y_k = CX_k + v \tag{20}$$

In the above equations X_k represents the system state vector at time instant k, T_s represents the sampling time, u_k represents the system input vector. It consists of thruster input, rudder and elevator deflections and w, v

are process and measurement noises respectively they are gaussian white noise processes having zero mean.

4. Airship Model Inaccuracy And Model Uncertainty Estimation

In case of model uncertainty estimation, for filter formulation the model state function and model measurement function are modified. Model uncertainty is incorporated by introducing six additional states. The modified state vector is given by.

$X =$

$[x \quad y \quad z \quad \phi \quad \theta \quad \psi \quad u \quad v \quad w \quad p \quad q \quad r \quad M_{u1} \quad M_{u2} \quad M_{u3} \quad M_{u4} \quad M_{u5} \quad M_{u6}]^T$

$\tag{21}$

For model uncertainty estimation it is assumed that the state estimation algorithm as explained in section 3 provides an estimate of position and attitude. This assumption leads to the following modified measurement vector.

$$Y = CX = \begin{bmatrix} 1 & 0 & 0 & 0 & 0 & 0 & 0 & 0 & 0 & 0 & 0 & 0 \\ 0 & 1 & 0 & 0 & 0 & 0 & 0 & 0 & 0 & 0 & 0 & 0 \\ 0 & 0 & 1 & 0 & 0 & 0 & 0 & 0 & 0 & 0 & 0 & 0 \\ 0 & 0 & 0 & 1 & 0 & 0 & 0 & 0 & 0 & 0 & 0 & 0 \\ 0 & 0 & 0 & 0 & 1 & 0 & 0 & 0 & 0 & 0 & 0 & 0 \\ 0 & 0 & 0 & 0 & 0 & 1 & 0 & 0 & 0 & 0 & 0 & 0 \end{bmatrix} X \tag{22}$$

5. Nonlinear Estimators Design

5.1 EKF for Airship State and Model Uncertainty Estimation

EKF is a nonlinear version of Kalman filter it consists of two steps: Prediction and correction. In prediction step system states and error covariance matrix for next sampling instant are predicted using system model and its Jacobian linearization respectively. In this step

process noise covariance matrix is utilized for the calculation of error covariance. Process noise covariance matrix is used as a tuning parameter. It is a diagonal matrix. Large weights are assigned to those elements whose modelling equations are unknown. In airship state estimation case Q is tuned after many iterations. In correction step, predicted state estimates are corrected using available sensor measurements and Kalman gain. Both main steps of EKF algorithm are further elaborated as follows:

5.1.1 Prediction

Step 1 First the nonlinear system model is used for the prediction of next state value.

$$\tilde{X}_{k+1} = f(\hat{X}_k, u_k) \tag{23}$$

Step 2 State Jacobian function and process noise covariance is used for the prediction of state error covariance.

$$\tilde{P}_{k+1} = \Phi_k \hat{P}_k \Phi_k^T + Q, \qquad \Phi_k = \frac{\partial f(\hat{X}_k, u_k)}{\partial X_k}\big|_{\hat{X}_k} \tag{24}$$

5.1.2 Correction

Step 3 EKF gain is calculated using predicted error covariance.

$$\tilde{K}_{k+1} = \tilde{P}_{k+1} C^T (C\tilde{P}_{k+1} C^T + R)^{-1} \tag{25}$$

Step 4 Sensor measurements and Kalman gain are used for the correction of states.

$$\hat{X}_{k+1} = \tilde{X}_{k+1} + \tilde{K}_{k+1}(Y - C\tilde{X}_{k+1}) \tag{26}$$

Step 5 Error covariance matrix is corrected.

$$\hat{P}_{k+1} = (I - \tilde{K}_{k+1} C)\tilde{P}_{k+1} \tag{27}$$

5.2 UKF For Airship State And Model Uncertainty Estimation

The main operation performed in Kalman filter algorithms is to propagate the gaussian random variable through the system dynamics. EKF algorithm approximate the state distribution by gaussian random variable. Which is then analytically propagated through nonlinear system's first order linearization. In UKF algorithm this problem is addressed by deterministic sampling approach. In which minimal set of sample points are carefully selected to propagate the state distribution by gaussian random variables. These sample point possess the characteristics of capturing the true mean and covariance of gaussian random variables. When they are passed through the actual nonlinear system then they capture the mean and covariance up to the third order Taylor series expansion for system nonlinearity. In UKF algorithm, in first step, set of state values are generated that are called sigma points. They capture the mean and covariance of state. The sigma points are used as an input to the state transition and measurement functions. The state transition and measurement functions return the transformed state points. And then state estimates are obtained from the mean and covariance of the transformed points. The next two sub sections summarize the correction and prediction steps of UKF algorithm.

5.2.1 Correction

Selection of sigma points

$$\hat{x}^{(0)}[k] = \hat{x}[k-1] \tag{28}$$
$$\hat{x}^{(i)}[k] = \hat{x}[k-1] + \Delta x^{(i)} \quad i = 1, \dots, 2M \tag{29}$$
$$\Delta x^{(i)} = \left(\sqrt{cP[k-1]}\right)_i \quad i = 1, \dots, M \tag{30}$$

$$\Delta x^{(M+i)} = -(\sqrt{cP[k-1]})_i \quad i = 1, \dots, M \tag{31}$$

Where, $c = \alpha^2(M + \kappa)$ is a scaling factor based on number of states M, and the parameters α and κ.

Using nonlinear measurement function for the calculation of predicted measurements

$$\hat{y}^{(i)}[k] = h(\hat{x}^{(i)}[k-1], u[k]) \quad i = 0,1,\dots,2M \tag{32}$$

Combining the predicted measurements to obtain the predicted measurement at time k.

$$\hat{y}[k] = \sum_{i=0}^{2M} w_M^i \hat{y}^i[k-1] \tag{33}$$

$$W_M^0 = 1 - \frac{M}{\alpha^2(M+\kappa)} \tag{34}$$

$$W_M^i = \frac{1}{2\alpha^2(M+\kappa)} \quad i = 1,2,\dots,2M \tag{35}$$

Estimating the covariance of predicted measurements, where $R[K]$ accounts for additive measurement noise.

$$P_y = \sum_{i=0}^{2M} w_c^i (\hat{y}^i[k-1] - \hat{y}[k])^T (\hat{y}^i[k-1] - \hat{y}[k])^T + R[k] \tag{36}$$

$$W_c^0 = (2 - \alpha^2 + \beta) - \frac{M}{\alpha^2(M+\kappa)} \tag{37}$$

$$W_c^i = \frac{1}{2\alpha^2(M+\kappa)} \quad i = 1,2,\dots,2M \tag{38}$$

Estimate the cross-covariance between $\hat{x}[k]$ and $\hat{y}[k]$.

$$P_{xy} = \frac{1}{2\alpha^2(M+\kappa)} \sum_{i=0}^{2M} w_c^i (\hat{x}^i[k-1] - \hat{x}[k-1])(\hat{y}^i[k-1] - \hat{y}[k])^T \tag{39}$$

The summation starts from i $= 1$ because $\hat{x}0[k-1] - \hat{x}[k-1] = 0$.

Obtaining the estimated state and state estimation error covariance at time step k.

$$K = P_{xy} P_y^{-1} \tag{40}$$

$$\hat{x}[k] = \hat{x}[k-1] + K(y[k] - \hat{y}[k]) \qquad (41)$$

$$P[k] = P[k-1] - KP_y K_k^T \qquad (42)$$

Here K is the Kalman gain.

5.2.2 Prediction

Choose the sigma points $x^i[k]$ at time step k.

$$\hat{x}^{(0)}[k] = \hat{x}[k] \qquad (43)$$

$$\hat{x}^{(i)}[k] = \hat{x}[k] + \Delta x^{(i)} \quad i = 1, \dots, 2M \qquad (44)$$

$$\Delta x^{(i)} = \left(\sqrt{cP[k]}\right)_i \quad i = 1, \dots, M \qquad (45)$$

$$\Delta x^{(M+i)} = -(\sqrt{cP[k]})_i \quad i = 1, \dots, M \qquad (46)$$

Using nonlinear system modelling equation for the calculation of predicted states for each sigma points

$$\hat{x}^{(i)}[k+1] = f(\hat{x}^{(i)}[k], u[k]) \qquad (47)$$

Combining the predicted states to obtain the predicted states at time k + 1.

$$\hat{x}[k+1] = \sum_{i=0}^{2M} w_M^i \hat{x}^{(i)}[k] \qquad (48)$$

$$W_M^0 = 1 - \frac{M}{\alpha^2(M+\kappa)} \qquad (49)$$

$$W_M^i = \frac{1}{2\alpha^2(M+\kappa)} \qquad i = 1,2,\dots,2M \qquad (50)$$

Computing the covariance of the predicted state. Adding $Q[k]$ to account for the additive process noise.

$$P[k+1] = \sum_{i=0}^{2M} w_c^i \left(\hat{x}^{(i)}[k] - \hat{x}[k]\right)^T \left(\hat{x}^{(i)}[k] - \hat{x}[k]\right)^T + Q[k] \qquad (51)$$

$$W_c^0 = (2 - \alpha^2 + \beta) - \frac{M}{\alpha^2(M+\kappa)} \qquad (52)$$

$$W_c^i = \frac{1}{2\alpha^2(M+\kappa)} \qquad i = 1,2,\dots,2M \qquad (53)$$

5.3 PF For Airship State Estimation

Unscented and extended Kalman filters aim to track the mean and covariance of the posterior distribution of the state estimates by different approximation methods. While the particle filter tracks the evolution of many state hypotheses (particles) over time, at the expense of higher computational cost. The computational cost and estimation accuracy increase with the number of particles. It is a recursive, Bayesian state estimator that uses discrete particles to approximate the posterior distribution of an estimated state. The particle filter algorithm computes the state estimates recursively and involves initialization, prediction, and correction steps. The detail algorithmic steps of the particle filter can be found in [42-45].

6. Results and Discussion

6.1 Simulation Scenario

For validating the estimator performances, simulations have been performed. For this study nonlinear 6-DOF simulation model for 'UETT Airship' has been developed. UETT airship project was started in the University of Engineering and Technology Taxila (UETT), Pakistan in 2013. In our previous work the parameters of the airship are provided in Table 1. Open loop simulations are performed in which thruster input, elevator and rudder deflections are given to the airship in specific time intervals. It is assumed that airship weight and buoyancy are equal, so neutral buoyancy condition is considered. Operating at 100 m of altitude, after 3 seconds of simulation run a thruster input is applied. Due to the application of thruster it starts moving in the forward direction with some 'u' velocity as shown in Fig. 2 (i). From Fig 2 (ii) it can be seen that initially the airship has zero sway velocity but after 20 seconds of flight as the rudder deflection is applied, it changes to 0.3 ms-1 and returns to its initial value when rudder input is removed after 40 s. Application of this input also changes yaw rate as well as yaw angle, as can be seen in Fig. 3 and 4 respectively. For evaluating the response of estimators, an elevator deflection case is also incorporated. Due to this input, changes in vertical velocity, pitch rate and pitch angle happen. Elevator deflection is applied after 40 s of flight time. Fig. 2 (iii) shows that initially its value is zero but due to the application of input it changes to 0.6 ms-1 and comes down to zero when the input is removed at 50 s. Effect of elevator deflection on pitch rate and pitch angle can be seen in Fig. 3 (ii) and 4 (ii) respectively. In order to evaluate the steady state response of estimators, after 90 s of flight once again rudder deflection is applied. This time it is applied for 30 s. Due to its application it changes the sway velocity, yaw rate and yaw angle that can be seen in Figs. 2-4 respectively.

Table 1

Parameters of Airship

Length of Hull	9 m
Diameter of Hull	2.2 m
Volume of Hull	25 m3
Mass of Hull, gondola, fins and propellers	24.073 Kg
Moment of inertia I_x	2.842114 kg-m2
Moment of inertia I_y, I_z	26.769788 kg-m2
Product of inertia I_{xz}	0.001166 kg-m2

6.2 State Estimation Using Current Location Measurements Of Airship

Figs 2-4 also show the estimation of linear velocities and angular velocities in BFRF and attitude angles in IRF by EKF, UKF and PF. True and measured values are generated from the modelling equations of airship. In measured values process and measurement noise is considered while true values correspond to noise free data. All estimators are fed with thruster, rudder and elevator inputs and x; y and z measurement data corrupted with noise.

Fig 2 shows the estimation of linear velocities in body fixed reference frame. The response is zoomed in between 60 s to 60.04 s to show the performance of filters. It can be seen that the estimated values remain close to the true ones. Among the three filters, PF response overlaps while UKF response is close to true response and EKF shows a larger estimation error. Figs. 2 (ii), 3 (i) and 4 (i) show 'sway velocity', 'roll rate' and 'roll angle' respectively. It can be observed that the transient response of particle filter is oscillatory across true value and lasts for 10 s but after that achieves its steady state value and remain close to the true value. The key parameter of interest used for validating the state estimation is the estimation error between true and estimated values. In this study we performed the error analysis of EKF, UKF and PF estimation for a single simulation run. In reality the true states are never available. In order to get the confidence on estimator's performances the error analysis should have small magnitude, zero mean and it should remain within a 1-σ uncertainty bound.

Figs 5-7 show the plots of error analysis of estimators for linear velocities, angular velocities and attitude angles. From these plots, it can be concluded that the estimators fulfill the minimum performance criteria because magnitudes of errors are small, and their means are close to zero. Fig 5 shows the plots for linear velocities. From the plo0ts it can be seen that error for all estimators remain within a 1-σ uncertainty bound. In zoomed-in portion from 60 s to 60.04 s black line indicates the desired error value. The portion shows that PF and UKF estimation error is close to zero while EKF estimation error is larger than PF and UKF. The same sort of error curves can be seen in Figs 6 and 7 for angular velocities estimation and Euler angle estimation. Mean estimation errors according to the Eq 55 is calculated for all estimated states and are given in Table 2.

$$Mean\ estimation\ error = \frac{1}{N}\sum_{i=0}^{i=t}(True\ value\ (i) - Estimated\ Value(i)) \quad (54)$$

where, t is the total simulation time and N, is the total number of samples. From Table 2 it can be observed that PF bring about maximum of 89 % decrease in mean estimation error than EKF as in case of θ state and minimum of 1.24 % decrease as in case of ψ state. UKF bring about maximum of 40 % decrease in mean estimation error as in case of v state and minimum of 0.15% decrease as in case of r state. The table data shows that Performance of all filters are reasonable but PF and UKF perform superior to the EKF.

Table 2

Mean Estimation error of ekf, ukf and pf for state estimation

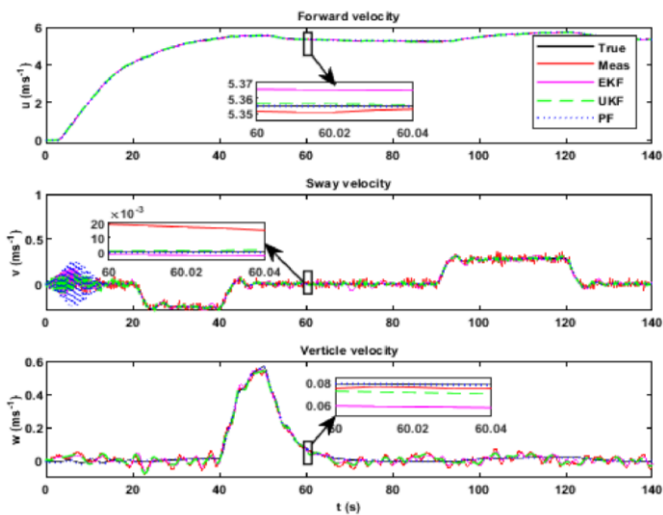| State	Mean estimation error		
	EKF	UKF	PF
ϕ (roll angle)	0.0001	0.00003	0.000004
θ (pitch angle)	0.0026	0.0025	0.000029
ψ (yaw angle)	0.0761	0.00787	0.0061
u (forward velocity)	0.0113	0.0111	0.0020
v (sway velocity)	0.0004	0.00001	0.00001
w (vertical velocity)	0.0012	0.002	0.0004
P (roll rate)	0.0003	0.0002	0.00004
q (pitch rate)	0.001	0.0008	0.0001
r (yaw rate)	0.0006	0.0019	0.0001

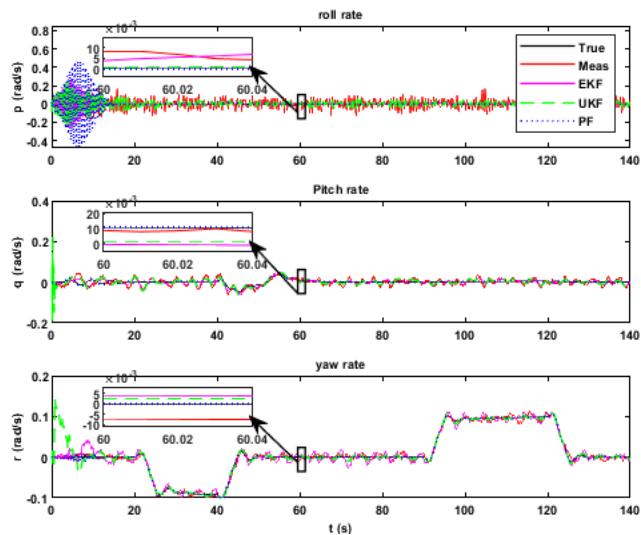**Fig. 2.** Comparisons of EKF, UKF and PF for Linear velocity estimation

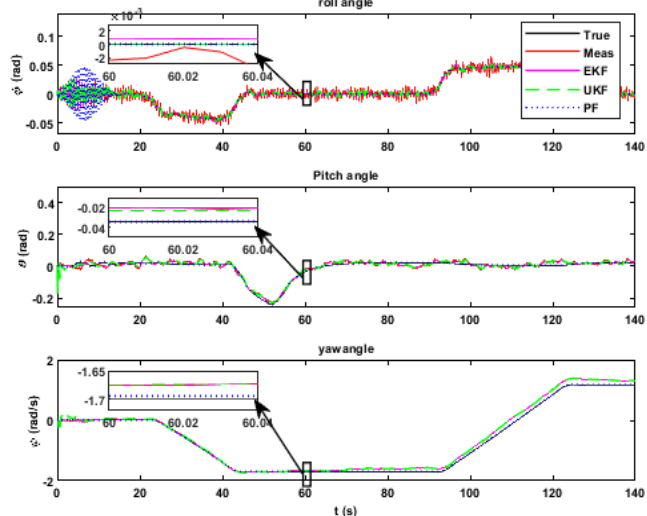**Fig. 3.** Comparisons of EKF, UKF and PF for Angular velocity estimation

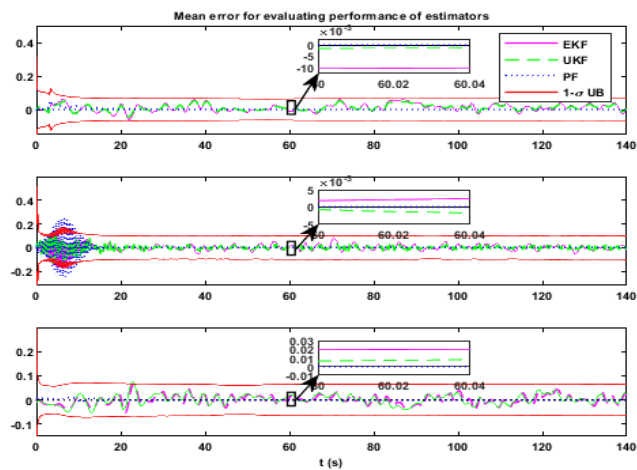**Fig. 4.** Comparisons of EKF, UKF and PF for Euler angle estimation

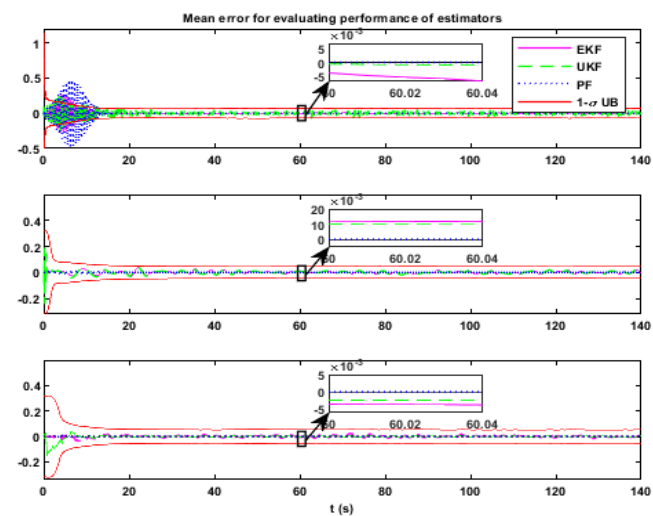**Fig. 5.** EKF, UKF and PF performance analysis for Linear velocity estimation

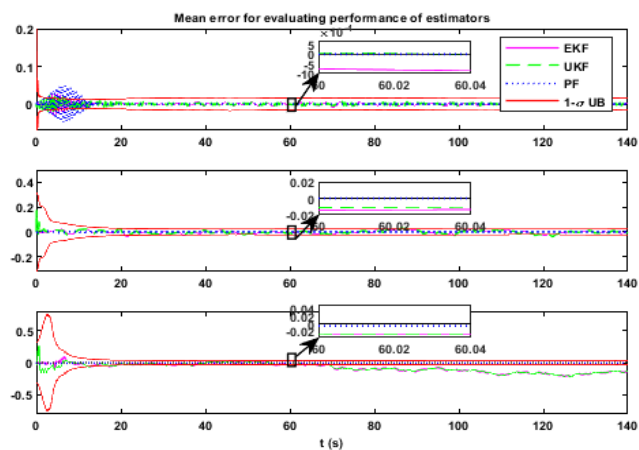**Fig. 6.** EKF, UKF and PF performance analysis for Angular velocity estimation

Fig. 7. EKF, UKF and PF performance analysis for Euler angle estimation

6.3 Model Uncertainties and State Estimation Using Current Location And Current Attitude Measurements Of Airship

For evaluating the estimator performance in case of model uncertainty, same open loop simulation scheme is adopted as discussed in the previous subsection. However, in this case change in aerodynamic forces has been introduced after 10 s and lumped approach is adopted for estimating its cumulative effect (sec 3.1). In this case EKF and UKF have been designed. Model inputs in the form of thruster, rudder and elevator deflections and output measurements including current airship coordinates x, y, z and current airship attitudes ϕ, θ, ψ are applied to the filter. Filter estimates model inaccuracies and model uncertainties and linear and angular velocities of the airship.

Figs 8 and 9 show the measured states by estimators and Figs 10 and 11 show the estimation of model uncertainties. Fig 8 shows the linear velocities plots, that are zoomed for 60 s to 60.04 s to quantify the individual performances of estimators. It can be seen that UKF outperforms EKF in the case of estimating linear velocities. Only For evaluating the estimator performance in case of model uncertainty same open loop simulation scheme is adopted as discussed in previous section but after 10s of simulation run change in aerodynamic forces has been introduced and lumped approach is adopted for estimating its cumulative effect. In this case EKF and UKF has been designed. Model inputs in the form of thruster, rudder and elevator deflections and measurements inputs, current airship coordinates (x, y, z) and current airship attitude (ϕ, θ, ψ) are applied to the filter. Filter estimates linear and angular velocities of airship, model inaccuracies and model uncertainties. Figures 8 and 9 shows the measured states by estimators. And figures 10 and 11 shows the estimation change in model. Figure 8 shows the linear velocities plots, they are zoomed for 60s to 60.04s to quantify the individual performances of estimators. It can be seen that UKF outperforms then EKF in the case of estimating linear velocities.

Fig 9 shows the angular velocities plots. It can be seen that in case of estimating roll rate and yaw rate, performance of both the filters is same but in estimating pitch rate UKF slightly outperforms the EKF. Figs 10 and 11 show that in the case of estimating model uncertainty, the transient response of EKF is better than UKF but in steady state UKF outperforms the EKF. These observations show that in case of detecting faults EKF can be preferred. Same error analysis has been performed for evaluating estimator performances in the

case of state and model uncertainties estimation. True values have been generated and error between estimated and true values is calculated. Figs 12 and 13 show error analysis for linear and angular velocities estimation. These plots show that the error remains in 1-σ uncertainty bound implying that the estimators' performances are acceptable. The zoomed portion of the plot shows that UKF outperforms EKF. Fig 14 and 15 show the plots of error and 1-σ uncertainty bounds for estimation of model uncertainty for body fixed reference frame modelling equations of airship. These plots show that error remains within 1-σ uncertainty bound in this case also. Initially in transient state EKF performance is better than UKF but in steady state, UKF outperforms the EKF. In order to assess the cumulative performance of estimators, mean error has been calculated and given in Table 3 where δ_u correspond to the model uncertainty in u state.
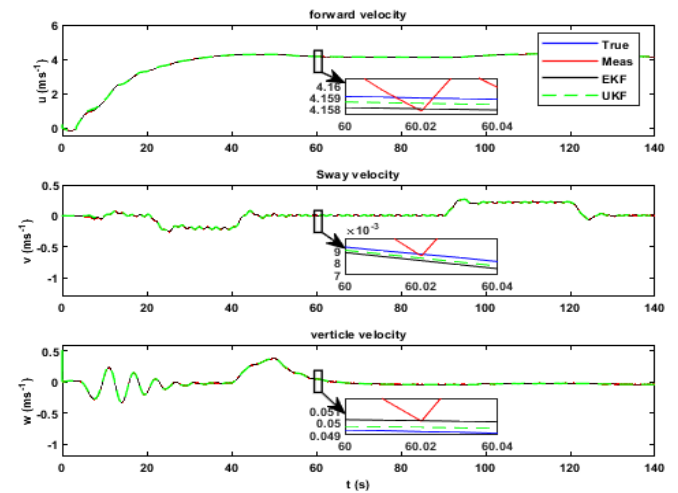

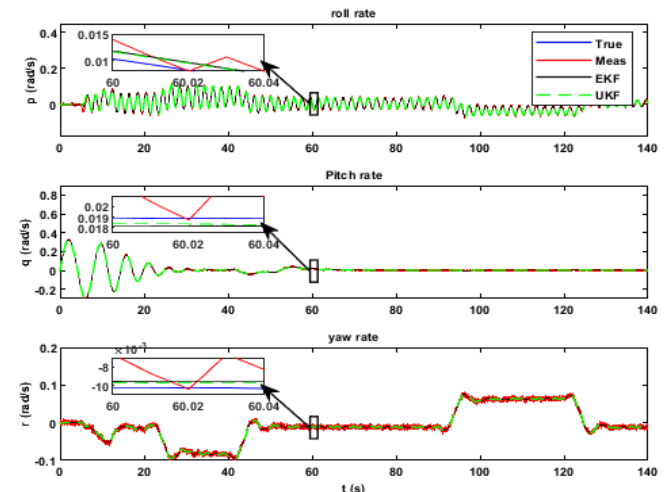**Fig. 8.** Comparisons of EKF and UKF for Linear velocity estimation

Fig. 9. Comparisons of EKF and UKF for Angular velocity estimation
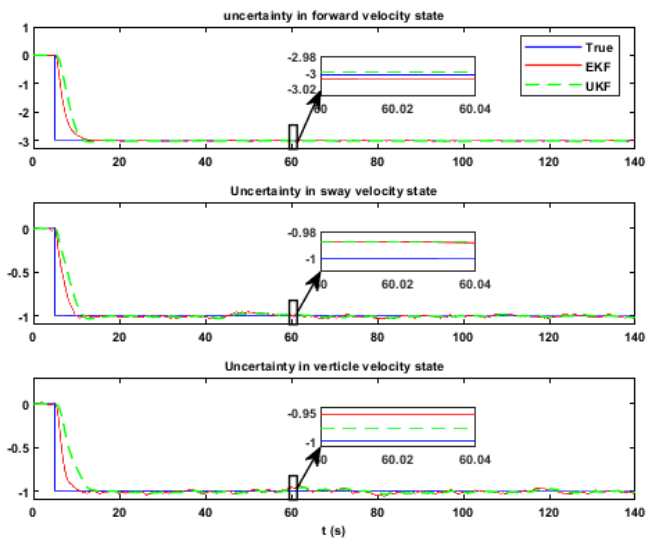
Fig. 10. Comparisons of EKF and UKF for model uncertainty estimation in total forces acting on airship in body axes
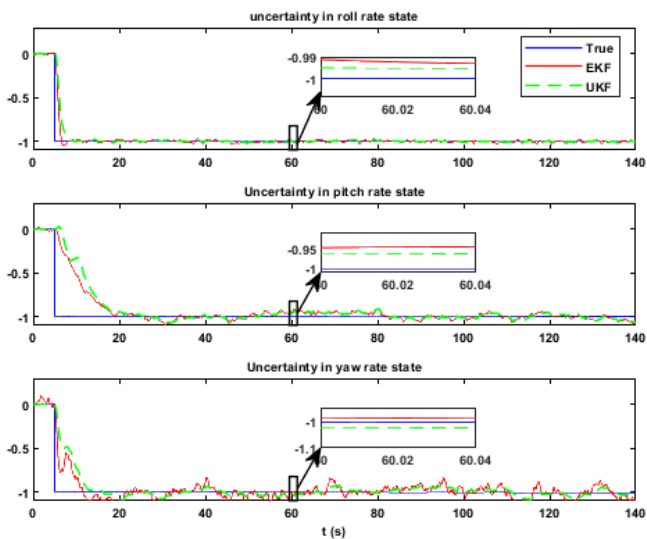

Fig. 11. Comparisons of EKF and UKF for model uncertainty estimation in total Torques acting on airship in body axes
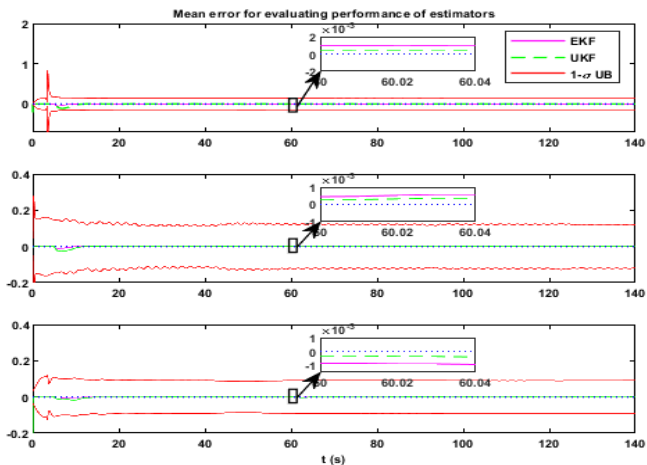

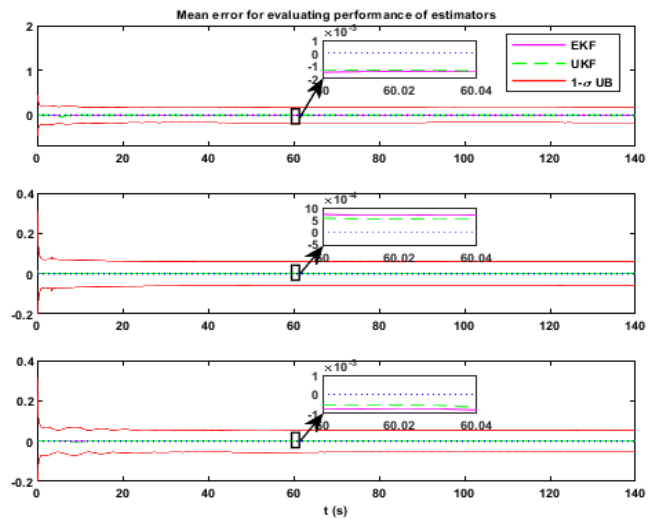**Fig. 12.** EKF and UKF performance analysis for Linear velocity estimation

Fig. 13. EKF and UKF performance analysis for Angular velocity estimation
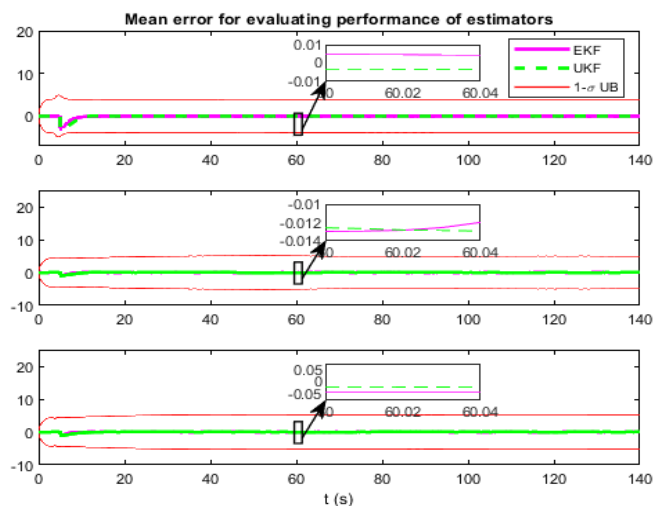

Fig. 14. Comparisons of EKF and UKF for model uncertainty estimation in total forces acting on airship in body axes
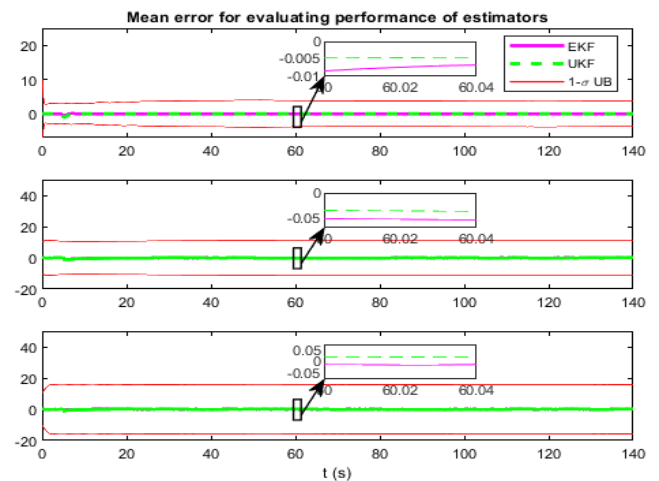

Fig. 15. Comparisons of EKF and UKF for model uncertainty estimation in total Torques acting on airship in body axes

Table 3

Mean estimation error of ekf, ukf and pf for state estimation

state	Mean estimation error	
	EKF	UKF
u (forward velocity)	0.0008	0.0027
v (sway velocity)	0.0002	0.0007
w (vertical velocity)	0.0002	0.0006
P (roll rate)	0.00227	0.00341
q (pitch rate)	0.00042	0.00021
r (yaw rate)	0.000085	0.000094
δ_u	0.0478	0.0680
δ_v	0.0120	0.0199
δ_w	0.0091	0.0233
δ_p	0.0065	0.0099
δ_q	0.0435	0.0533
δ_r	0.0123	0.0241

7. Conclusion

In this article the estimation of airship states and model uncertainty information with nonlinear and Bayesian estimators under minimum sensor measurements is addressed. Two problems have been addressed. In the first problem airship current coordinates are used as measurements and airship attitude and body axes linear and angular velocities are estimated. In this case EKF, UKF and PF are designed, and their individual performances are assessed. 1-σ uncertainty bound, and error analysis are performed for getting confidence on the estimator performances. Error analysis shows that PF's transient response is not satisfactory but in steady state it outperforms the EKF and UKF. As airship has slow dynamics, the transient response of particle filter can be deemed as acceptable. In the second problem airship body axes linear velocities and angular velocities and model uncertainties have been identified using EKF and UKF estimators. In this case, airship current coordinates and attitudes are considered as measurements for estimators. The study shows that EKF quickly responds to parameter change effect but in the steady state UKF outperform it. Error analysis is carried out that supports the observation.

8. Acknowledgement

9. References

[1] S. H. Miller, R. Fesen, L. Hillenbrand, J. Rhodes, G. Baird, G. Blake, J. Booth, D. E. Carlile, R. Duren, F. G. Edworthy, et al., "Airships: A new horizon for science," arXiv preprint arXiv:1402.6706, 2014.

[2] Chen, L., Dong, Q., Zhang, G., & Duan, D, "Composite control system of hybrid-driven mid-altitude airship". The Aeronautical Journal, 122(1248), 173-204, 2018.

[3] M. Alexandra, "Modeling and nonlinear control for airship autonomous flight." PhD Dissertation, Universidade Técnica de Lisboa, Lisbona, Grudzień, 2007.

[4] Y. Yang, J. Wu, and W. Zheng, "Adaptive fuzzy sliding mode control for robotic airship with model uncertainty and external disturbance," Journal of Systems Engineering and Electronics, vol. 23, no. 2, pp. 250–255, 2015.

[5] L. Cheng, Z. Zuo, J. Song, and X. Liang, "Robust three-dimensional path-following control for an under-actuated stratospheric airship," Advances in Space Research, vol. 63, no. 1, pp. 526–538, 2019.

[6] S. Liu, S. Gong, Y. Li, and Z. Lu, "Vectorial backstepping method–based trajectory tracking control for an under-actuated stratospheric airship," The Aeronautical Journal, vol. 121, no. 1241, pp. 916–939, 2017.

[7] C. Nie, M. Zhu, Z. Zheng, and Z. Wu, "Model-free control for stratospheric airship based on reinforcement learning," in 35th Chinese Control Conference (CCC), pp. 10702–10707, IEEE, 2016.

[8] B. Neil, and G. Schmidt. "Inertial sensor technology trends." IEEE Sensors Journal 1.4: 332-339, 2001.

[9] L.Tao, G. Yuan, L. Wang, "Particle filter with novel nonlinear error model for miniature gyroscope-based measurement while drilling navigation," Sensors, 16, 371, 2016.

[10] G.G, Rigatos, "Nonlinear kalman filters and particle filters for integrated navigation of unmanned aerial vehicles," Robotics Auton. Syst, 60, 978–995, 2012.

[11] M. S. Persson, and I. Sharf, "Steady-state invariant Kalman filter for attitude and

imbalance estimation of a neutrally-buoyant airship." AIAA Guidance, Navigation, and Control (GNC) Conference, 2013.

[12] J. L. Crassidis, and F. L. Markley, "Unscented filtering for spacecraft attitude estimation." Journal of Guidance, Control, and Dynamics 26.4: 536-542, 2003.

[13] E. J. Lefferts, F. L. Markley, and M. D. Shuster, "Kalman filtering for spacecraft attitude estimation," AIAA Aerospace Sciences Meeting, Vol. 5, No. 5, pp. 417-429, 1982.

[14] J. L. Crassidis, F. L. Markley, and Y. Cheng, "Survey of nonlinear attitude estimation methods," Journal of Guidance, Control and Dynamics, Vol. 30, No. 1, pp. 12-28, 2007.

[15] H. Ramesh, N. K. Sinha, and P. Balasubramanian. " Design of Kalman Filter for Smooth State Estimation of Airship Dynamics" Proceedings of the. ISSE Conference on Large Scale Multi-disciplinary Systems of National Significance, 2016.

[16] B. Johan, and W. Steyn. "Kalman filter configurations for a low-cost loosely integrated inertial navigation system on an airship." Control Engineering Practice 16.12: 1509-1518, 2008.

[17] A. Ghassan, and K. Subbarao, "Guidance, navigation and control of unmanned airships under time-varying wind for extended surveillance." Aerospace 3.1: 8, 2016.

[18] S. Leonardo, and S. Lacroix, "Airship control." Multiple Heterogeneous Unmanned Aerial Vehicles. Springer, Berlin, Heidelberg. 147-188, 2007.

[19] Y. Yin, "Nonlinear Control and State Estimation of Holonomic Indoor Airship," McGill University (Canada), 2012.

[20] Wasim, M., & Ali, A, "Estimation of Airship Aerodynamic Forces and Torques Using Extended Kalman Filter". IEEE Access, 8, 70204-70215, 2020.

[21] W. Muhammad, and A. Ahsan, "Airship aerodynamic model estimation using unscented Kalman filter". Journal of Systems Engineering and Electronics, 31(6), pp.1318-1329, 2020.

[22] W. Muhammad, and A. Ahsan, M. A. Choudhry, F. Saleem, I. U. H. Shaikh, & J. Iqbal, "Unscented Kalman filter for airship model uncertainties and wind disturbance estimation". Plos One, 16(11), e0257849, 2021.

[23] M. Jörg, O. Paul, and W. Burgard, "Probabilistic velocity estimation for autonomous miniature airships using thermal air flow sensors." IEEE International Conference on Robotics and Automation. IEEE, 2012.

[24] M. Jörg, and W. Burgard, "Efficient probabilistic localization for autonomous indoor airships using sonar, air flow, and IMU sensors," Advanced Robotics 27.9: 711-724, 2013.

[25] Z. Gao, D. Mu, Y. Zhong, & C. Gu, "Constrained unscented particle filter for SINS/GNSS/ADS integrated airship navigation in the presence of wind field disturbance," Sensors, 19(3), 471, 2019.

[26] J. Wang, and M. Xiuyun, "Active disturbance rejection backstepping control for trajectory tracking of the unmanned airship." IEEE International Conference on Unmanned Systems. IEEE, 2017.

[27] O. A. Choudhry, W. Muhammad, A. Ali, M. A. Choudhry, & J. Iqbal, "Modelling and robust controller design for an underactuated self-balancing robot with uncertain parameter estimation," Plos One, 18(8), e0285495, 2023.

[28] W. X. Zhou, P. F. Zhou, Y. Y. Wang, & D. P. Duan, "Planar path following nonlinear controller design for an autonomous airship," Proceedings of the Institution of Mechanical Engineers, Part G: Journal of Aerospace Engineering, 233(5), 1879-1899, 2019.

[29] C. Xiao, D. Han, Y. Wang, P. Zhou, & D. Duan, "Fault-tolerant tracking control for a multi-vectored thrust ellipsoidal airship using adaptive integral sliding mode approach," Proceedings of the Institution of Mechanical Engineers, Part G: Journal of Aerospace Engineering, 232(10), 1911-1924, 2018.

[30] C. Xiao, Y. Wang, P. Zhou, & D. Duan, "Adaptive sliding mode stabilization and positioning control for a multi-vectored thrust airship with input saturation considered," Transactions of the Institute of Measurement and Control, 40(15), 4208-4219, 2018.

[31] Y. Yue-neng, J. Wu, and W. Zheng, "Trajectory tracking for an autonomous airship using fuzzy adaptive sliding mode control." Journal of

Zhejiang University SCIENCE C 13.7: 534-543, 2012.

[32] Y. Yueneng, and Y. Yan, "Trajectory tracking for robotic airships using sliding mode control based on neural network approximation and fuzzy gain scheduling." Proceedings of the Institution of Mechanical Engineers, Part I: Journal of Systems and Control Engineering 230.2: 184-196, 2016.

[33] Y. Yueneng, W. Wang, and Y. Yan, "Adaptive backstepping neural network control for three dimensions trajectory tracking of robotic airships." CEAS Aeronautical Journal 8.4: 579-587, 2017.

[34] Y. Yueneng, and Y. Yan, "Neural network approximation-based nonsingular terminal sliding mode control for trajectory tracking of robotic airships." Aerospace Science and Technology 54: 192-197, 2016.

[35] Z. Zewei, and Y. Zou, "Adaptive integral LOS path following for an unmanned airship with uncertainties based on robust RBFNN backstepping." ISA Transactions 65: 210-219, 2016.

[36] S. Yu, G. Xu, K. Zhong, S. Ye, & W. Zhu, "Direct-adaptive fuzzy predictive control for path following of stratospheric airship," 29th Chinese Control And Decision Conference, pp. 5658-5664, 2017.

[37] Y. Yueneng, J. Wu, and W. Zheng, "Station-keeping control for a stratospheric airship platform via fuzzy adaptive backstepping approach." Advances in Space Research 51.7: 1157-1167, 2013.

[38] Y. Yang, Y. Yan, Z. Zhu, & W. Zheng, "Positioning control for an unmanned airship using sliding mode control based on fuzzy approximation," Proceedings of the Institution of Mechanical Engineers, Part G: Journal of Aerospace Engineering, 228(14), 2627-2640, 2014.

[39] L. Yuwen, M. Nahon, and I. Sharf, "Airship dynamics modeling: A literature review." Progress in Aerospace Sciences 47.3: 217-239, 2011.

[40] M. Z. Ashraf, and M. A. Choudhry, "Dynamic modeling of the airship with Matlab using geometrical aerodynamic parameters."

Aerospace Science and Technology 25.1: 56-64, 2013.

[41] A. Mansoor, and A. C. Mohammad, "System identification of an airship using trust region reflective least squares algorithm." International Journal of Control, Automation and Systems 15.3: 1384-1393, 2017.

[42] K. Emami, T. Fernando, H. H. C. Iu, H. Trinh, & K. P. Wong, "Particle filter approach to dynamic state estimation of generators in power systems," IEEE Transactions on Power Systems, 30(5), 2665-2675, 2014.

[43] Z. Yang, S. McWilliam, A. A. Popov, and T. Hussain, "A probabilistic approach to variation propagation control for straight build in mechanical assembly," International Journal of Advanced Manufacturing Technology, Vol. 64(5-8), p. 1029-1047, 2013.

[44] T. Hussain, S. McWilliam, A. A. Popov, and Z. Yang, "Geometric error reduction in the assembly of axi-symmetric rigid components - a 2d case study," Proceedings of the Institution of Mechanical Engineers, Part B, Journal of Engineering Manufacture, Vol. 226(7), p. 1259-1274, 2012.

[45] M. Memon, T. Hussain, and, Z. Ali, "Minimizing assembly errors by selecting optimum assembly sequence in the assembly of rigid circular structure," Mehran University Research Journal of Engineering and Technology, Vol. 31(4): 743-754, 2012.